

Observation of Floquet Raman transition in a driven solid-state spin system

Zijun Shu,^{1,2,*} Yu Liu,^{1,2,*} Qingyun Cao,^{1,2} Pengcheng Yang,^{1,2}

Shaoliang Zhang,^{1,2,†} Martin B. Plenio,^{3,2} Fedor Jelezko,^{4,2} and Jianming Cai^{1,2,‡}

¹*School of Physics, Huazhong University of Science and Technology, Wuhan 430074, China*

²*International Joint Laboratory on Quantum Sensing and Quantum Metrology, Huazhong University of Science and Technology, Wuhan, 430074, China*

³*Institut für Theoretische Physik & IQST, Albert-Einstein Allee 11, Universität Ulm, D-89081 Ulm, Germany*

⁴*Institut für Quantenoptik & IQST, Albert-Einstein Allee 11, Universität Ulm, D-89081 Ulm, Germany*

(Dated: December 14, 2024)

We experimentally observe Floquet Raman transitions in the weakly driven solid state spin system of nitrogen-vacancy center in diamond. The periodically driven spin system simulates a two-band Wannier-Stark ladder model, and allows us to observe coherent spin state transfer arising from Raman transition mediated by Floquet synthetic levels. It also leads to the prediction of analog photon-assisted Floquet Raman transition and dynamical localisation in a driven two-level quantum system. The demonstrated rich Floquet dynamics offers new capabilities to achieve effective Floquet coherent control of a quantum system with potential applications in various types of quantum technologies based on driven quantum dynamics. In particular, the Floquet-Raman system may be used as a quantum simulator for the physics of periodically driven systems.

PACS numbers: 76.30.Mi, 76.70.Hb, 07.55.Ge

Introduction.— Coherent control of quantum system is an essential prerequisite in a wide range of quantum experiments [1, 2]. In particular, it is the most fundamental ingredient for the realization of quantum technology, including quantum computing [3], quantum simulation [4, 5] and quantum sensing [6]. Time-dependent periodic driving, as implemented for example by laser and microwave field, is commonly used for coherent quantum control of atom and spin systems [7, 8]. For two-level quantum systems, the well known Rabi oscillation [9] induced by a weak periodic driving field on resonance leads to coherent oscillatory state transitions. Stimulated Raman transitions between two ground states via a far detuned third excited state provide an extremely powerful tool for coherent manipulation [10]. Moreover, periodic driving is an useful tool that may lead to new exotic phases, such as topological Floquet insulators [12–16] and time crystals [17–20]. An important consequence of periodic driving is the emergence of synthetic dimensions supported by Floquet dressed state which opens the field of Floquet Hamiltonian engineering [21] and new techniques for coherent quantum control [22].

Periodic driving is not only the basis of coherent quantum control, it also plays an important role in several fundamental concepts in quantum dynamics, e.g. geometric phase [23] and adiabatic quantum algorithm, where the validity of adiabatic evolution [24–29] is usually required. The traditional adiabatic condition requires the change of Hamiltonian to be sufficiently slow on the time scale that is proportional to the inverse squared energy gap [9]. Such an adiabatic condition was however found to be neither sufficient nor necessary to guarantee adiabaticity [30–35]. An observation of non-adiabaticity violating the traditional adiabatic condition was shown in [36] which

can be explained by Rabi resonance. The general anomalous non-adiabaticities appearing in a weakly periodically driven two-level system has fundamental connection with Floquet resonance [39]. The experimental demonstration of general anomalous non-adiabaticities in periodically driven systems remains challenging due to the requirement of sufficiently long coherence time and precise quantum control.

In this work, we experimentally study Floquet dynamics of a single nitrogen-vacancy (NV) center spin in diamond driven by a *weak* microwave field. As compared with strong driving [22], the driving strength is much weaker than the frequency detuning and conventionally it would not induce spin state transition. With such a weakly driven two-level system, we simulate a two band Wannier-Stark ladder model [37, 38], and instead observe coherent oscillation between spin states. The phenomenon represents Raman transition between Floquet synthetic levels [39] albeit the system itself is a two-level quantum system. We also show that analog photon-assisted Raman transition can be realised among Floquet levels, which provides a new knob for the engineering of quantum control. We expect that the present idea can be extended to simulate and investigate variants of Wannier-Stark ladder model, e.g. with complex hopping amplitudes, by exploiting Floquet synthetic levels. In addition, the observed Floquet Raman transitions manifest general anomalous non-adiabaticities in periodically driven system, and may help to gain further insight into adiabatic quantum dynamics.

Floquet Raman transition.— The two-level quantum system in our experiment is a spin- $\frac{1}{2}$ system from the subspace of the triplet ground state manifold of a single NV center in electronic grade bulk diamond (with less than 5

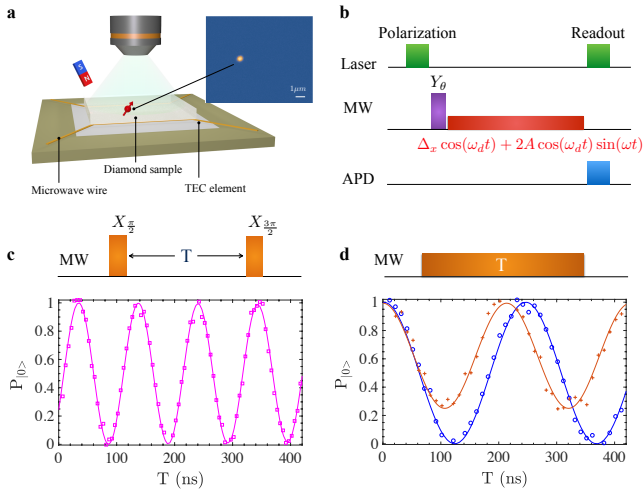


Figure 1. (Color online) Setup for observation of Floquet Raman transition of NV center spin in diamond. (a) Schematic representation of the experimental setup. The temperature of the diamond sample is stabilized by a TEC element. The NV center spin is coupled to the microwave driving field via a copper wire waveguide. The readout of the NV center spin state is achieved by spin-dependent fluorescence. Confocal scan image of an NV center is shown in the inset. (b) Pulse sequence for Floquet Raman transition. MW corresponds to the microwave field, and the optical measurement is performed by a photodetector (APD). The initial spin state is prepared with a microwave pulse Y_θ (rotation around \hat{y} axis by angle θ), the duration of which is $\tau = \theta/2\Omega$ where Ω is the amplitude of the microwave pulse. The synthesized microwave driving field $V(t) = \Delta_x \cos(\omega_d t) + 2A \cos(\omega_d t) \sin(\omega t)$ implements Floquet quantum control. (c) shows Ramsey measurement, the oscillation of which allows us to determine the frequency detuning Δ_z . (d) shows Rabi oscillations with two driving frequencies ($\omega_d/2\pi = 1445.8$ MHz (blue, \circ) and 1443.8 MHz (red, $+$). Measurement of the effective Rabi frequency $\omega_0 = (\Delta_z^2 + \Delta_x^2)^{1/2}$ gives an estimation of the driving amplitude $\Delta_x = (2\pi)4.06$ MHz.

ppb nitrogen impurities). The scan image of NV center as shown in Fig.1(a) is obtained from a home-built confocal setup. The NV center spin has the advantage of long coherence time (i.e. narrow line broadening) under ambient condition [40], which is mainly dependent on the nuclear spin bath in diamond and temperature fluctuation for the present sample. The NV center has a triplet ground state with three spin sublevels $m_s = 0, \pm 1$. The degeneracy of $m_s = \pm 1$ is lifted by applying an external magnetic field B_z along the NV axis, which provides an effective two-level system supported by the ground state sublevels $m_s = 0$ and $m_s = -1$ with an energy gap $\Delta E = D - \gamma B_z$, where the zero field splitting is $D = (2\pi)2.87$ GHz and γ is the electron gyromagnetic ratio. We apply a magnetic field $B_z = 509$ G along the NV axis so that the nitrogen nuclear spin is polarized. The value of ΔE is determined by pulsed optically detected magnetic resonance

measurement (pulsed ODMR), which also confirms the polarization of the nitrogen nuclear spin [41]. The stability of the energy splitting is very critical to observe Floquet Raman transition [39]. In our experiment setup, we mount the diamond sample on a single-stage TEC element under temperature control. The temperature of the diamond sample is stabilized by a 12W temperature controller (Thorlabs TED200C) so that the temperature fluctuation is reduced down to 0.1K that corresponds to a line broadening of ~ 7.7 kHz [42]. The Ramsey measurement suggests a line broadening of ~ 40 kHz for the NVs used in our experiment, which corresponds to a coherence time of $T_2^* \simeq 4\mu s$, see Fig.1(c).

To implement Floquet quantum control and observe Floquet Raman transition, we synthesize a microwave field described by $V(t) = \Delta_x \cos(\omega_d t) + 2A \cos(\omega_d t) \sin(\omega t)$ with $\Delta_x, A \ll \omega_d$ with accurate timing and amplitude by using a Tektronics arbitrary waveform generator. In the interaction picture, we find the effective Hamiltonian for the two-level system [41]

$$H = \frac{\Delta_z}{2} \sigma_z + \frac{\Delta_x}{2} \sigma_x + A \sin(\omega t) \sigma_x, \quad (1)$$

where we set $\hbar = 1$, $\Delta_z = \Delta E - \omega_d$, σ_x, σ_z are Pauli operators for the spin- $\frac{1}{2}$ system, Δ_x and Δ_z represent the transversal and longitudinal components of the energy splitting. In our experiment, we exploit Floquet synthetic levels supported by the periodically driven Hamiltonian in Eq.(1) to achieve coherent control of spin state. To precisely determine the relevant parameters, we perform Ramsey measurement and determine the frequency detuning Δ_z , see Fig.1(c). Subsequently, we measure Rabi oscillation and estimate the effective Rabi frequency $\omega_0 = (\Delta_x^2 + \Delta_z^2)^{1/2}$, see Fig.1(d), from which we are able to determine Δ_x . We are interested in the weak driving and large detuning limit, namely $A \ll |\omega_0 - \omega|$, where ω_0 quantifies the energy gap between the eigenstates of $H_s = (\Delta_z/2)\sigma_z + (\Delta_x/2)\sigma_x$. We remark that the Floquet Hamiltonian Eq.(1) is also feasible by applying a magnetic field that has both longitudinal and transversal components (namely Δ_z and Δ_x).

According to Floquet theory, the evolution dynamics of the periodically driven two-level system can be described by Floquet quasi energy states (namely Floquet modes) $|\phi_k(t)\rangle$ with the corresponding quasienergy ϵ_j as $|\Psi(t)\rangle = \sum_k c_k e^{-i\epsilon_k t} |\phi_k(t)\rangle$. The Floquet states and spectrum were observed in a strongly driven superconducting flux qubit [22]. The Floquet dynamics of a weakly driven two-level system can be mapped to a two-band Wannier-Stark ladder model [37–39]. The upper and lower bands arising from Floquet synthetic dimensions [20] correspond to the spin states $|\pm\rangle$ that are the eigenstates of H_s [41], namely $|+\rangle = \cos(\frac{\theta}{2})|0\rangle + \sin(\frac{\theta}{2})|-1\rangle$ and $|-\rangle = -\sin(\frac{\theta}{2})|0\rangle + \cos(\frac{\theta}{2})|-1\rangle$ with $\theta = \tan^{-1}(\Delta_x/\Delta_z)$. The energies of the upper and lower Floquet levels denoted as $|\pm, n\rangle$ are $E_{\pm, n} = \pm(\omega_0/2) + n\omega$, where \pm repre-

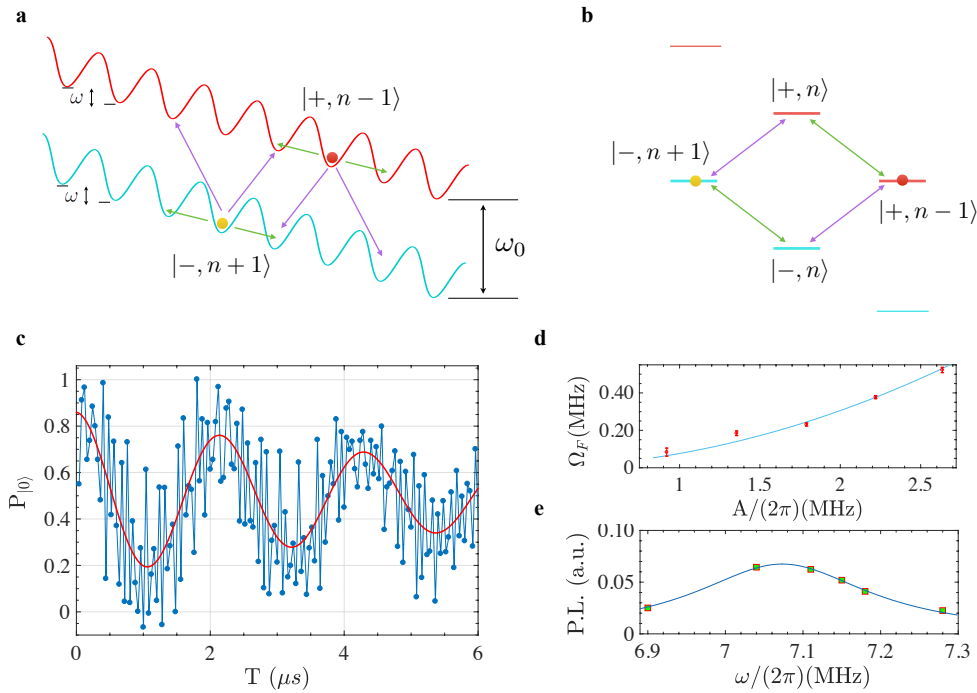


Figure 2. (Color online) Floquet Raman transition of NV center spin in diamond. **(a)** A two band Wannier-Stark ladder model is simulated by a periodically driven spin- $\frac{1}{2}$ system. The energy gap between the upper and lower band is ω_0 , and the ladder energy spacing is given by the frequency ω of the weak driving field. The arrows represent couplings between Floquet synthetic levels. **(b)** Raman transition between the lower and upper band levels $|-, n+1\rangle$ and $|+, n-1\rangle$ is mediated by Floquet synthetic levels $|+, n\rangle$ and $|-, n\rangle$. **(c)** Coherent spin state transfer is realized by Floquet Raman transition. The strength and frequency of the weak microwave driving field are $A = (2\pi)2.37$ MHz and $\omega = (2\pi)6.985$ MHz. The other parameters are $\Delta_z = (2\pi)10.03$ MHz, and $\Delta_x = (2\pi)9.67$ MHz. **(d)** The dependence of Floquet Raman transition Rabi frequency Ω_F on the driving strength A , as compared with the numerical simulation result (cyan curve). The parameters are $\omega = (2\pi)7.09$ MHz, $\Delta_z = (2\pi)9.92$ MHz, and $\Delta_x = (2\pi)10.12$ MHz. **(e)** The contrast of Floquet Raman transition as a function of the driving frequency ω . The parameters are $A = (2\pi)1.37$ MHz, $\Delta_z = (2\pi)9.63$ MHz, and $\Delta_x = (2\pi)10.32$ MHz.

sents the upper and lower band respectively, see Fig.2(a). As $|\pm\rangle$ are not the eigenstates of σ_x , the effect of the weak driving field as written in the Hamiltonian Eq.(1) will couple the levels $|\alpha, n\rangle$ with $|\beta, n \pm 1\rangle$, where $\alpha, \beta = \pm$, see Fig.2(a). The strength of such off-resonant coupling is $(A/2\omega_0)[\delta_{\alpha\beta}\Delta_x + (1 - \delta_{\alpha\beta})\Delta_z]$ [39, 41]. Therefore, it can be seen that the transition between the upper and lower band as mediated by Floquet levels can be exploited to manipulate spin state in a coherent manner.

In our experiment, we exploit the three-level configurations provided by Floquet synthetic levels, allowing the implementation of Raman transitions between the upper and lower levels. For example, $|+, n-1\rangle$, $|-, n+1\rangle$ and $|+, n\rangle$ ($|-, n\rangle$) forms a Λ (V) three-level configuration, see Fig.2(b). In order to enable efficient far-detuned Raman transition between $|+, n-1\rangle$ and $|-, n+1\rangle$ via the intermediate states $|\pm, n\rangle$, the energy resonant condition has to be satisfied, namely $E_{+,n-1} = E_{-,n+1}$ [39, 41]. This leads to the Floquet resonance condition $\omega = (\omega_0/2)$, which contrasts to the conventional Rabi resonance condition $\omega = \omega_0$ for a driven two-level system [39]. The resonance conditions are slightly modified due to higher-

order dynamical Stark shifts [39]. We first prepare the NV center spin in the state $|+\rangle$, namely in the upper band, by applying a microwave pulse on resonance with the two-level system with the amplitude Ω for a time duration $\tau_\theta = \theta/(2\Omega)$ to induce a rotation of angle θ around \hat{y} axis. The system is then governed by the Floquet Hamiltonian as in Eq.(1) arising from the microwave driving field $V(t)$, see Fig.1(b). We measure the state population of the spin level $|0\rangle$ as a function of the evolution time. As shown in Fig.2(c), our experimental data clearly demonstrates Floquet Raman transition between the upper and lower band. Under the resonant condition, the state population $P_{|0\rangle}$ can be written as $P_{|0\rangle} = \frac{1}{2}[1 + \cos\theta \cos(\Omega_F t) - \sin\theta \sin(\Omega_F t) \sin(\omega_0 t)]$ [41], where Ω_F is the Rabi frequency induced by Floquet Raman transition. We remark that the additional fast oscillation feature is mainly due to the interband energy splitting ω_0 , and can be eliminated by an additional appropriate microwave pulse [41]. We further characterize the dependence of the Rabi frequency of the Floquet Raman transition on the driving strength A , see Fig.2(d),

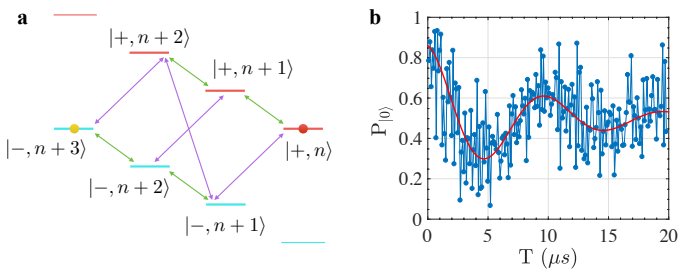


Figure 3. (Color online) Third-order Floquet Raman transition between the lower and upper band levels $|-, n+3\rangle$ and $|+, n\rangle$. (a) The Raman transition is mediated by multiple intermediate levels $|\pm, n+1\rangle$ and $|\pm, n+2\rangle$. (b) The state $|0\rangle$ population as a function of time demonstrates coherent Raman Floquet transition of the spin state as realized by a third-order Floquet resonance. The frequency of the weak microwave driving field is $\omega = (2\pi)4.657$ MHz, and the other parameters are $A = (2\pi)2.37$ MHz, $\Delta_z = (2\pi)9.82$ MHz, $\Delta_x = (2\pi)9.67$ MHz.

which agrees well with the theoretical analysis and numerical simulation $\Omega_F = 2A^2\Delta_x\Delta_z/\omega_0^3$ [41]. In Fig.2(e), we show the relative contrast of Floquet Raman transition which clearly demonstrates Floquet resonant feature, namely an optimal Raman transition efficiency appears when the resonant condition is satisfied.

Raman transition between the other Floquet synthetic levels are also feasible if the general m -th order Floquet resonance condition $\omega = (\omega_0/m)$ is satisfied [39], where Floquet Raman transition is mediated by multiple levels [43, 44], see Fig.3(a). In our experiment, we tune the frequency of the weak microwave driving field to match the third-order Floquet resonance condition $\omega = (\omega_0/3)$. The coherent oscillation of the spin state population as shown in Fig.3(b) demonstrates the third-order Floquet resonance enabled Raman transition. The observed Rabi frequency of Floquet Raman transition is estimated to be $\Omega_F = 9A^3\Delta_x^2\Delta_z/(2\omega_0^5)$ which agrees well with Floquet theory [39]. The observed Floquet Raman transition allows to coherently manipulate spin state using a driving field with under-limited frequency, and thus may facilitate coherent quantum control e.g. under a high magnetic field. We remark that the parameters that allow us to observe resonant spin state transition in our experiment satisfy the traditional adiabatic condition [41]. Nevertheless, the spin system does not follow an adiabatic evolution trajectory, and instead demonstrates evident state transition. The phenomenon is not discovered in the previous relevant experiment [36], and represents more general anomalous non-adiabaticities in weakly driven systems.

Analog photon-assisted Floquet Raman transition.— The observed Floquet-Raman transition is a high-order process due to the energy gap between upper and lower band. According to Floquet theory, we predict

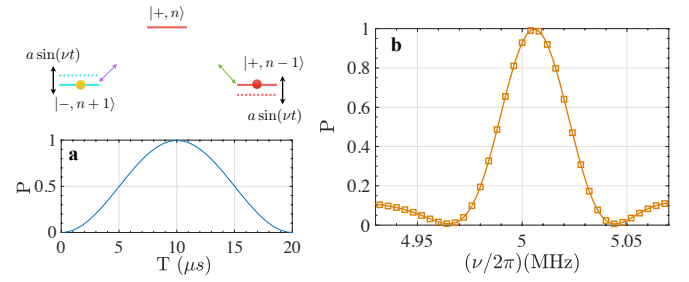


Figure 4. (Color online) Analog photon-assisted Floquet Raman transition between the lower and upper band levels $|-, n+1\rangle$ and $|+, n-1\rangle$, the energies of which are harmonically modulated at a frequency of ν . (a) The transition probability P from $|-, n+1\rangle$ to $|+, n-1\rangle$ in a second-order Floquet Raman transition. (b) The transition probability P at time $T = 2.5\mu\text{s}$ as a function of the modulation frequency ν . The amplitude of the frequency modulation is $a = (2\pi)0.24$ MHz. The other parameters are $\omega = (2\pi)10.015$ MHz, $A = (2\pi)0.5$ MHz, and $\Delta_z = \Delta_x = (2\pi)14.142$ MHz.

that the speed of Floquet-Raman transition can be enhanced by a frequency modulated driving field $V_d(t) = A \sin[\omega t + a \sin(\nu t)]$. In the Floquet picture, the frequency modulation leads to the oscillating of Floquet levels, see Fig.4. This allows for the experimental examination of photon-assisted tunnelling [45, 46], resonance enhanced quantum transport [47] and probe for coherence in driven systems [48], as it causes k -photon assisted (Floquet) Raman transition with an enhanced transition rate $\sim \mathcal{J}_k(\frac{a}{\nu})$ [41] when $k\nu = \omega$, where $\mathcal{J}_n(x)$ is the n -th order Bessel function, or dynamical localisation for zeros of this Bessel function [47, 49]. Although the Floquet energy structure in the present scenario is more complicated than a Λ system, it still exhibits the analog of photon-assisted enhancement in transition efficiency. In Fig.4(a-b), it can be seen that an analog two-photon assisted Floquet-Raman transition ($\nu = \omega/2$) with a small amplitude of frequency modulation ($a/\omega = 0.024$) can achieve a complete state transfer requiring a time that is significantly reduced. This result thus offers a new perspective to engineer quantum control of a driven two-level quantum system.

Conclusion.— To summary, we simulate a two-band Wannier-Stark ladder model using a solid state spin system under weak periodic driving. We exploit the synthetic dimensions in the Floquet framework and experimentally observe second- and third-order Raman transition mediated by Floquet synthetic levels. We show that analog photon-assisted Floquet Raman transition may exist in such a driven two-level quantum system. The present result enriches Floquet dynamics for Floquet Hamiltonian engineering aiming for the development of new techniques for coherent quantum control and the investigation of novel Floquet quantum phases. In addition, the observed Floquet Raman transition provides

additional and more general scenarios which violate the widely adopted traditional adiabatic condition, and may provide insights into adiabatic dynamical evolution of quantum systems.

Acknowledgements – We thank Dr. A. Russomanno, H.-B. Liu and J.-F. Wang for helpful discussions. The work is supported by National Natural Science Foundation of China (11690030, 11690032, 11574103), National 1000 Youth Talent Program, Huazhong University of Science and Technology. M. B. P. is supported by the DFG (FOR1493), the EU STREPs DIADEMS and HYPERDIAMOND, and the ERC Synergy grant BioQ. F. J. acknowledge support from DFG (FOR 1493, SPP 1923), VW Stiftung, BMBF, ERC, EU (DIADEMS), BW Stiftung, Ministry of Science and Arts, Center for Integrated quantum science and technology (IQST).

* These authors contributed equally to this work.

† shaoliang@hust.edu.cn

‡ jianmingcai@hust.edu.cn

- [1] R. J. Gordon, A. R. Stuart, *Annu Rev Phys Chem.* **48**, 601 (1997).
- [2] M. Shapiro, P. Brumer, *Advances In Atomic, Molecular, and Optical Physics* **42**, 287 (2000).
- [3] M. A. Nielsen, I. L. Chuang, *Quantum Computation and Quantum Information* (2nd ed.), Cambridge University Press. (2010).
- [4] R. P. Feynman, *Int. J. Theor. Phys.* **21**, 467 (1982).
- [5] S. Lloyd, *Science* **273**, 1073 (1996).
- [6] C. L. Degen, F. Reinhard, and P. Cappellaro, *Rev. Mod. Phys.* **89**, 035002 (2017).
- [7] L. M. K. Vandersypen and I. L. Chuang, *Rev. Mod. Phys.* **76**, 1037 (2005).
- [8] R. Blatt and D. J. Wineland, *Nature* **453**, 1008 (2008).
- [9] J. J. Sakurai, Jim J. Napolitano, *Modern Quantum Mechanics (2nd Edition)*, World Book Press (2011).
- [10] B. W. Shore, *Multilevel Atoms and Incoherence*, The Theory of Coherent Atomic Excitation, Vol. 2 (John Wiley & Sons, New York, 1990).
- [11] T. Kitagawa, E. Berg, M. Rudner, and E. Demler, *Phys. Rev. B* **82**, 235114 (2010).
- [12] N. H. Lindner, G. Refael, and V. Galitski, *Nature Physics* **7**, 490 (2011).
- [13] M. S. Rudner, N. H. Lindner, E. Berg, and M. Levin, *Phys. Rev. X* **3**, 031005 (2013).
- [14] M. C. Rechtsman, J. M. Zeuner, Y. Plotnik, Y. Lumer, D. Podolsky, F. Dreisow, S. Nolte, M. Segev, A. Szameit, *Nature* **496**, 196 (2013).
- [15] D. A. Abanin, W. De Roeck, and F. Huveneers, *Annals of Physics* **372**, 1 (2016).
- [16] H. Wang, L. Zhou and J. Gong, *Phys. Rev. B* **91**, 085420 (2015).
- [17] N. Y. Yao, C. R. Laumann, S. Gopalakrishnan, M. Knap, M. Müller, E. A. Demler, and M. D. Lukin, *Phys. Rev. Lett.* **113**, 243002 (2014).
- [18] S. Choi, J. Choi, R. Landig, G. Kucsko, H. Zhou, J. Isoya, F. Jelezko, S. Onoda, H. Sumiya, V. Khemani, C. von Keyserlingk, N. Y. Yao, E. Demler, M. D. Lukin, *Nature* **543**, 221 (2017).
- [19] J. Zhang, P. W. Hess, A. Kyprianidis, P. Becker, A. Lee, J. Smith, G. Pagano, I.-D. Potirniche, A. C. Potter, A. Vishwanath, N. Y. Yao, and C. Monroe, *Nature* **543**, 201 (2017).
- [20] I. Martin, G. Refael, and B. Halperin, *Phys. Rev. X* **7**, 041008 (2017).
- [21] N. Goldman and J. Dalibard, *Phys. Rev. X* **4**, 031027 (2014).
- [22] C. Deng, J.-L. Orgiazzi, F. Shen, S. Ashhab, and A. Lupascu, *Phys. Rev. Lett.* **115**, 133601 (2015).
- [23] M. V. Berry, *Proc. R. Soc. London A* **392**, 45 (1984).
- [24] P. Ehrenfest, *Ann. Phys* **356**, 327 (1916).
- [25] M. Born and V. Fock, *Z. Phys.* **51**, 165 (1928).
- [26] T. Kato, *J. Phys. Soc. Jpn.* **5**, 435 (1950).
- [27] W. H. Zurek, U. Dorner and P. Zoller, *Phys. Rev. Lett.* **95**, 105701 (2005).
- [28] J. Brooke, D. Bitko, T. F. Rosenbaum and G. Aeppli, *Science* **284**, 779 (1999).
- [29] E. Farhi, J. Goldstone, S. Gutmann, J. Lapan, A. Lundgren and D. Preda, *Science* **292**, 472 (2001).
- [30] K.-P. Marzlin and B. C. Sanders, *Phys. Rev. Lett.* **93**, 160408 (2004).
- [31] D. M. Tong, K. Singh, L. C. Kwek, and C. H. Oh, *Phys. Rev. Lett.* **95**, 110407 (2005).
- [32] D. M. Tong, K. Singh, L. C. Kwek, and C. H. Oh, *Phys. Rev. Lett.* **98**, 150402 (2007).
- [33] D. M. Tong, *Phys. Rev. Lett.* **104**, 120401 (2010).
- [34] Dafa Li and Man-Hong Yung, *New J. Phys.* **16** 053023 (2014).
- [35] Z.-Y. Wang, M. B. Plenio, *Phys. Rev. A* **93**, 052107 (2016).
- [36] J.-F. Du, L.-Z. Hu, Y. Wang, J.-D. Wu, M.-S. Zhao, and D. Suter, *Phys. Rev. Lett.* **101**, 060403 (2008).
- [37] E. E. Mendez and G. Bastard, *Physics Today* **46**, 6, 34 (1981).
- [38] G. Grosso and G. P. Parravicini, *Solid State Physics*, Academic, San Diego (2000).
- [39] A. Russomanno, G. E. Santoro, *J. Stat. Mech.* **2017**, 103104 (2017).
- [40] M. W. Doherty, N. B. Manson, P. Delaney, F. Jelezko, J. Wrachtrup, L. C. L. Hollenberg, *Phys. Rep.* **528**, 1 (2013).
- [41] More detailed analysis and experimental data is included in supplementary information.
- [42] V. M. Acosta, E. Bauch, M. P. Ledbetter, A. Waxman, L.-S. Bouchard, and D. Budker *Phys. Rev. Lett.* **104**, 070801 (2010).
- [43] C. Cohen-Tannoudji, J. Dupont-Roc and G. Grynberg, *Atom-Photon Interactions: Basic Processes and Applications* (John Wiley & Sons 1992).
- [44] J. Bateman, A. Xuereb, and T. Freegarde, *Phys. Rev. A* **81**, 043808 (2010).
- [45] A. Eckardt, T. Jinasundera, C. Weiss, and M. Holthaus, *Phys. Rev. Lett.* **95**, 200401 (2005).
- [46] C. Sias, H. Lignier, Y. P. Singh, A. Zenesini, D. Ciampini, O. Morsch, and E. Arimondo, *Phys. Rev. Lett.* **100**, 040404 (2008).
- [47] A. Vaziri and M. B. Plenio, *New J. Phys.* **12**, 085001 (2010).
- [48] J. Almeida, P. de Groot, S. F. Huelga, A. Ligouri and M. B. Plenio. *J. Phys. B* **46**, 104002 (2013).
- [49] D. H. Dunlap and V. M. Kenkre, *Phys. Rev. B* **34**, 3625 (1986).

Supplementary Information: Observation of Floquet Raman transition in a driven solid-state spin system

Zijun Shu,^{1,2,*} Yu Liu,^{1,2,*} Qingyun Cao,^{1,2} Pengcheng Yang,^{1,2}
Shaoliang Zhang,^{1,2,†} Martin B. Plenio,^{3,2} Fedor Jelezko,^{4,2} and Jianming Cai^{1,2,‡}

¹*School of Physics, Huazhong University of Science and Technology, Wuhan 430074, China*

²*International Joint Laboratory on Quantum Sensing and Quantum Metrology,
Huazhong University of Science and Technology, Wuhan, 430074, China*

³*Institut für Theoretische Physik & IQST, Albert-Einstein Allee 11, Universität Ulm, D-89081 Ulm, Germany*

⁴*Institut für Quantenoptik & IQST, Albert-Einstein Allee 11, Universität Ulm, D-89081 Ulm, Germany*

Derivation of the effective Hamiltonian

By applying a microwave driving field as follows

$$V(t) = \Delta_x \cos(\omega_d t) + 2A \cos(\omega_d t) \sin(\omega t), \quad (\text{S.1})$$

the system Hamiltonian in the the lab frame can be written as follows

$$H_o = \frac{\Delta E}{2} \sigma_z + \Delta_x \cos(\omega_d t) \sigma_x + 2A \cos(\omega_d t) \sin(\omega t) \sigma_x, \quad (\text{S.2})$$

where ΔE is the energy of the two-level system. Here, the microwave field is designed to drive the transition between the spin sublevels $|0\rangle$ and $|-1\rangle$, while the other level $|+1\rangle$ is far detuned. Therefore, we can concentrate on the Hilbert subspace as spanned by $\{|0\rangle, |-1\rangle\}$, and σ_x and σ_z are Pauli operators of such an effective two-level system. In the interaction picture with respect to $H_0 = (\omega_d/2) \sigma_z$, we get the following Hamiltonian as

$$H_I = \frac{\Delta_z}{2} \sigma_z + \frac{\Delta_x}{2} \sigma_x + A \sin(\omega t) \sigma_x + \frac{\Delta_x}{2} [\cos(2\omega_d t) \sigma_x - \sin(2\omega_d t) \sigma_y] + A [\cos(2\omega_d t) \sigma_x - \sin(2\omega_d t) \sigma_y] \sin(\omega t), \quad (\text{S.3})$$

where $\Delta_z = \Delta E - \omega_d$. In our experiment, the condition $\omega, A, \Delta_x \ll \omega_d$ is satisfied. Therefore, under rotating wave approximation, we get the following effective Hamiltonian as implemented in the experiment

$$H = \frac{\Delta_z}{2} \sigma_z + \frac{\Delta_x}{2} \sigma_x + A \sin(\omega t) \sigma_x, \quad (\text{S.4})$$

that allows us to observe Floquet Raman transition in the synthetic dimensions.

Determination of experiment parameters

In order to determine the resonance frequency accurately, we first perform pulsed optically detected magnetic resonance (pulsed ODMR) measurement. The pulsed ODMR experiment, as shown in Fig.S1, exhibits one single

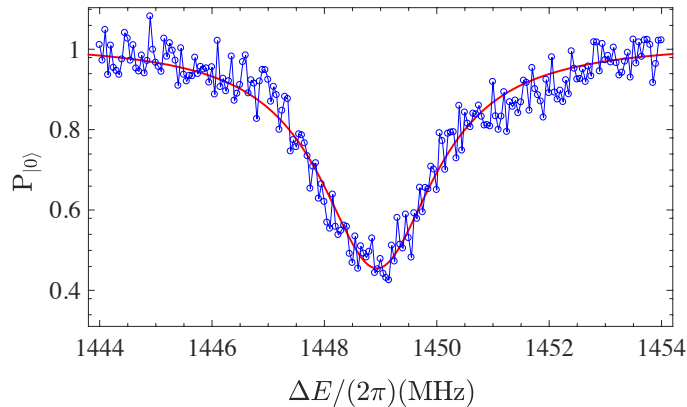


Figure S1: (Color online) The measurement of pulsed ODMR experiment gives an estimation of the resonance frequency 1448.9MHz, which corresponds a magnetic field around 508Gauss in parallel with the NV axis. The microwave pulse length is 500 ns with a Rabi frequency $\Omega \simeq (2\pi)1$ MHz.

resonant frequency with a finite linewidth, which confirms the polarization of the nitrogen nuclear spin associated with the NV center. To determine the frequency detuning Δ_z of the microwave driving field, we perform Ramsey experiment and determine the value of Δ_z from the oscillation frequency of Ramsey fringe, as shown in Fig.1(c) of the main text. The value of Δ_x is determined from the measurement of Rabi oscillation. Given a frequency detuning of Δ_z , the effective Rabi frequency is $\omega_0 = (\Delta_x^2 + \Delta_z^2)^{1/2}$, from which we can infer the parameter Δ_x .

Theoretical analysis of Floquet Raman transition

The presence of Floquet resonance in the present model was proposed in Ref.[1]. In this section, we provide theoretical analysis to elaborate our experiment observation of Floquet Raman transition. The evolution of a periodically driven system can be described in the framework of Floquet theory as

$$|\Psi(t)\rangle = \sum_k c_k e^{-i\epsilon_k t} |\phi_k(t)\rangle, \quad (\text{S.5})$$

where $|\phi_k(t)\rangle = \sum_{n=-\infty}^{\infty} |\phi_{k,n}\rangle e^{in\omega t}$ are Floquet states with the corresponding quasienergy ϵ_k . Considering a two-level system as governed by the Hamiltonian in Eq.(S.4), its dynamical evolution is governed by Schrödinger equation

$$i\frac{\partial}{\partial t}|\Psi(t)\rangle = H(t)|\Psi(t)\rangle. \quad (\text{S.6})$$

This leads to the following equation

$$i\partial_t|\phi_{k,n}(t)\rangle = \left(n\omega + \frac{\Delta_z}{2}\sigma_z + \frac{\Delta_x}{2}\sigma_x\right)|\phi_{k,n}(t)\rangle + \left(\frac{A}{2}\right)\sigma_x(|\phi_{k,n-1}(t)\rangle + |\phi_{k,n+1}(t)\rangle), \quad (\text{S.7})$$

here we use a translation $t \rightarrow t + \pi/(2\omega)$. The system can be mapped to a two-band Wannier-Stark ladder model with a tilted field ω [2]. We denote the unitary rotation around \hat{y} axis $U = \exp(i\theta\sigma_y/2)$, with $\theta = \tan^{-1}(\Delta_x/\Delta_z)$, which diagonalizes $H_s = (\Delta_z/2)\sigma_z + (\Delta_x/2)\sigma_x$, namely $UH_sU^\dagger \rightarrow \sigma_z$. Under such a transformation, Eq.(S.7) can be rewritten as follows [1].

$$i\partial_t|\tilde{\phi}_{k,j}(t)\rangle = \left(n\omega + \frac{\omega_0}{2}\sigma_z\right)|\tilde{\phi}_{k,n}(t)\rangle + \left(\frac{A}{2}\right)U\sigma_xU^\dagger(|\tilde{\phi}_{k,n-1}(t)\rangle + |\tilde{\phi}_{k,n+1}(t)\rangle), \quad (\text{S.8})$$

$$= \left(n\omega + \frac{\omega_0}{2}\sigma_z\right)|\tilde{\phi}_{k,n}(t)\rangle + \left(\frac{A}{2}\right)\left(\frac{\Delta_z}{\omega_0}\sigma_x + \frac{\Delta_x}{\omega_0}\sigma_z\right)(|\tilde{\phi}_{k,n-1}(t)\rangle + |\tilde{\phi}_{k,n+1}(t)\rangle) \quad (\text{S.9})$$

where $|\tilde{\phi}_{k,n}(t)\rangle = U|\phi_{k,n}(t)\rangle$ and $\omega_0 = \sqrt{\Delta_z^2 + \Delta_x^2}$. Therefore, it can be seen that the upper and lower band correspond to the spin state $|\pm\rangle = U^\dagger|0, 1\rangle$ that are the eigenstates of H_s , i.e.

$$|+\rangle = \cos\left(\frac{\theta}{2}\right)|0\rangle + \sin\left(\frac{\theta}{2}\right)|1\rangle, \quad (\text{S.10})$$

$$|-\rangle = -\sin\left(\frac{\theta}{2}\right)|0\rangle + \cos\left(\frac{\theta}{2}\right)|1\rangle. \quad (\text{S.11})$$

Using the basis $|n, +\rangle = |+\rangle e^{in\omega t}$ and $|n, -\rangle = |-\rangle e^{in\omega t}$, the Hamiltonian in paper can be translated into the following effective two-leg lattice model

$$\begin{aligned} \mathcal{H} = & \sum_{n,\sigma} \left(n\omega + \frac{\omega_0}{2}\sigma_z\right)|n, \sigma\rangle\langle\sigma, n| + \frac{A\Delta_x}{2\omega_0} \sum_n (|n, +\rangle\langle n+1, +| - |n, -\rangle\langle n+1, -| + h.c.) \\ & + \frac{A\Delta_z}{2\omega_0} \sum_n (|n, +\rangle\langle n+1, -| + |n, -\rangle\langle n+1, +| + h.c.). \end{aligned} \quad (\text{S.12})$$

The energies of the Floquet synthetic levels $|\pm, n\rangle$ (as shown in Fig.2a of the main text) are $E_{\pm, n} = \pm(\omega_0/2) - n\omega$. The second and third terms in Eq.(S.9) shows the coupling between the Floquet synthetic levels. If the interband tunneling can be ignored, the system is a two-leg Wannier-Stark ladder model. These two ladders can be diagonalized as follows

$$\mathcal{H}_{\text{intra}} = \sum_{m,\sigma} \left(\frac{\omega_0}{2}\sigma_z + m\omega\right)|\Psi_{m,\sigma}\rangle\langle\Psi_{m,\sigma}|, \quad (\text{S.13})$$

where

$$\begin{aligned} |\Psi_{m,+}\rangle &= \sum_n \mathcal{J}_{m-n} \left(\frac{A\Delta_x}{\omega_0\omega} \right) |n,+\rangle & |n,+\rangle &= \sum_m \mathcal{J}_{m-n} \left(\frac{A\Delta_x}{\omega_0\omega} \right) |\Psi_{m,+}\rangle \\ |\Psi_{m,-}\rangle &= \sum_n \mathcal{J}_{n-m} \left(\frac{A\Delta_x}{\omega_0\omega} \right) |n,-\rangle & |n,-\rangle &= \sum_m \mathcal{J}_{n-m} \left(\frac{A\Delta_x}{\omega_0\omega} \right) |\Psi_{m,-}\rangle. \end{aligned} \quad (\text{S.14})$$

With the new basis, the interband Hamiltonian can be expanded as

$$\begin{aligned} \mathcal{H}_{\text{inter}} &= \frac{A\Delta_z}{2\omega_0} \sum_n (|n,+\rangle\langle n+1,-| + |n,-\rangle\langle n+1,+| + h.c.) \\ &= \frac{\Delta_z\omega}{2\Delta_x} \left\{ \sum_{m,m'} \left[(m-m') \mathcal{J}_{m-m'} \left(\frac{2A\Delta_x}{\omega_0\omega} \right) \right] |\Psi_{m,+}\rangle\langle\Psi_{m',-}| + h.c. \right\}, \end{aligned} \quad (\text{S.15})$$

From the effective interaction Hamiltonian (S.15), if $A \ll \omega$ and any other energy scales, the amplitude of tunneling term is very small. So the tunneling is forbidden except for the case $\epsilon_{m,+} = \epsilon_{m',-}$. Consider the dynamical process. If the initial state is prepared on the $|0,+\rangle$ state, it can be written in the new basis as

$$|0,+\rangle = \sum_m \mathcal{J}_m \left(\frac{A\Delta_x}{\omega_0\omega} \right) |\Psi_{m,+}\rangle, \quad (\text{S.16})$$

when $A \ll \omega$, one can use the approximation $|0,+\rangle \approx |\Psi_{0,+}\rangle$. In the following, we consider two cases of Floquet resonance.

(1). 2^{nd} -order Floquet resonance: $\omega = \omega_0/2$. In this case, the resonance condition is $\epsilon_{m,+} = \epsilon_{m+2,-}$. The effective Hamiltonian is

$$\mathcal{H}_{\text{eff}}^{[2]} = -\frac{\Delta_z\omega}{\Delta_x} \mathcal{J}_2 \left(\frac{2A\Delta_x}{\omega_0\omega} \right) (|\Psi_{0,+}\rangle\langle\Psi_{2,-}| + h.c.) \approx -\frac{A^2\Delta_z\Delta_x}{2\omega_0^2\omega} (|\Psi_{0,+}\rangle\langle\Psi_{2,-}| + h.c.) \quad (\text{S.17})$$

In our experiment, we choose $\Delta_x \simeq \Delta_z$ to optimise the transfer efficiency, as seen from the above equation. There are other off-resonant transitions, e.g. one can extend the Hilbert space including three basis $|\Psi_{0,+}\rangle$, $|\Psi_{1,-}\rangle$ and $|\Psi_{2,-}\rangle$ as

$$\begin{aligned} \mathcal{H}_{\text{eff}}^{[2]} &= -\frac{\Delta_z\omega}{\Delta_x} \mathcal{J}_2 \left(\frac{2A\Delta_x}{\omega_0\omega} \right) (|\Psi_{0,+}\rangle\langle\Psi_{2,-}| + h.c.) + \frac{\Delta_z\omega}{2\Delta_x} \mathcal{J}_1 \left(\frac{2A\Delta_x}{\omega_0\omega} \right) (|\Psi_{0,+}\rangle\langle\Psi_{1,-}| + h.c.) - \omega |\Psi_{1,-}\rangle\langle\Psi_{1,-}| \\ &\approx -\frac{A^2\Delta_z\Delta_x}{2\omega_0^2\omega} (|\Psi_{0,+}\rangle\langle\Psi_{2,-}| + h.c.) + \frac{A\Delta_z}{2\omega_0} (|\Psi_{0,+}\rangle\langle\Psi_{1,-}| + h.c.) - \omega |\Psi_{1,-}\rangle\langle\Psi_{1,-}|. \end{aligned} \quad (\text{S.18})$$

The second term of this effective Hamiltonian describes off-resonant transition which may lead to fast oscillation. Its effect is suppressed when the energy detuning between two states $|\Psi_{0,+}\rangle$, $|\Psi_{1,-}\rangle$ satisfies the condition $\omega \gg (A\Delta_z/2\omega_0)$.

(2). 3^{rd} -order Floquet resonance: $\omega = \omega_0/3$. In this case, the resonance condition is $\epsilon_{m,+} = \epsilon_{m+3,-}$. The effective Hamiltonian is

$$\mathcal{H}_{\text{eff}}^{[3]} = \frac{3\Delta_z\omega}{2\Delta_x} \mathcal{J}_3 \left(\frac{2A\Delta_x}{\omega_0\omega} \right) (|\Psi_{0,+}\rangle\langle\Psi_{3,-}| + h.c.) \approx \frac{A^3\Delta_z\Delta_x^2}{4\omega_0^3\omega^2} (|\Psi_{0,+}\rangle\langle\Psi_{3,-}| + h.c.) \quad (\text{S.19})$$

It can be seen that the transfer efficiency is optimized when $\Delta_z \simeq \Delta_x/\sqrt{2}$. In our experiment, the system is initialized into the $|+\rangle$ state, and the state evolution is described as follows

$$|\psi(t)\rangle = \exp(-i\sigma_x\Omega_F t/2) |+\rangle = \cos\left(\frac{\Omega_F t}{2}\right) |+\rangle - i \sin\left(\frac{\Omega_F t}{2}\right) |-\rangle, \quad (\text{S.20})$$

where

$$2^{\text{nd}}\text{-order Floquet resonance: } \Omega_F = \left(\frac{A^2\Delta_z\Delta_x}{\omega_0^2\omega} \right) = \left(\frac{2A^2\Delta_z\Delta_x}{\omega_0^3} \right) \quad (\text{S.21})$$

$$3^{\text{rd}}\text{-order Floquet resonance: } \Omega_F = \left(\frac{A^3\Delta_z\Delta_x^2}{2\omega_0^3\omega^2} \right) = \left(\frac{9A^3\Delta_z\Delta_x^2}{2\omega_0^5} \right) \quad (\text{S.22})$$

represents the Rabi frequency of Floquet Raman transitions as see from Eq.(S.17-S.19), and $|+\rangle = \cos(\frac{\theta}{2})|0\rangle + \sin(\frac{\theta}{2})|1\rangle$, $|-\rangle = -\sin(\frac{\theta}{2})|0\rangle + \cos(\frac{\theta}{2})|1\rangle$, where $\theta = \tan^{-1}(\Delta_x/\Delta_z)$. Therefore, it can be seen that a complete state transfer between the spin states $|+\rangle$ and $|-\rangle$ can be achieved, and applying an additional rotation (U) around \hat{y} axis, one can implement coherent transition between the spin states $|m_s = 0\rangle$ and $|m_s = -1\rangle$. In the lab frame, the state evolution is

$$|\psi_s(t)\rangle = \cos\left(\frac{\Omega_F t}{2}\right) \exp\left(-i\frac{\omega_0}{2}t\right) |+\rangle - i \sin\left(\frac{\Omega_F t}{2}\right) \exp\left(i\frac{\omega_0}{2}t\right) |-\rangle. \quad (\text{S.23})$$

After the evolution for time T , we directly measure the population of the state $|m_s = 0\rangle$ via spin-dependent fluorescence, which can be written as follows

$$P_{|0\rangle} = |\langle 0|\psi_s(T)\rangle|^2 \quad (\text{S.24})$$

$$= \frac{1}{2} [1 + \cos(\theta) \cos(\Omega_F T) - \sin(\theta) \sin(\Omega_F T) \sin(\omega_0 T)]. \quad (\text{S.25})$$

The second term $\sim \sin(\omega_0 T)$ in Eq.(S.25) represent a fast oscillating feature, which agrees well with our experiment observation.

Floquet Raman transition with different driving amplitudes

In our experiment, we tune the amplitude A of the weak driving microwave field, and investigate the dependence of Rabi frequency of Floquet Raman transition on the driving amplitude. In Fig.S2(a-b), we show the coherent spin state transfer via Floquet Raman transition that is driven by a microwave field with different amplitude A . The experiment results are in good agreement with numerical simulation as shown in Fig.S2(c-d). We estimate the effective Rabi frequency of Floquet Raman transition Ω_F , which agree well with the prediction of Floquet theory as shown in Eq.(S.21-S.22).

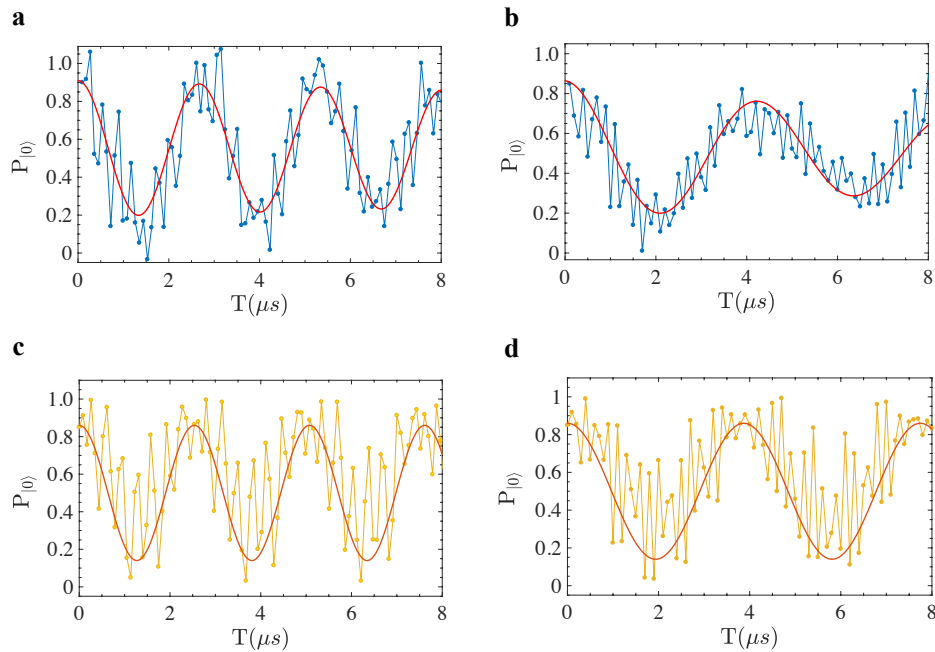


Figure S2: (Color online) Coherent spin state transfer via Floquet Raman transition that is driven by a microwave field with a frequency ω , and an amplitude of $A = (2\pi)2.22$ MHz (a), $(2\pi)1.79$ MHz (b), as compared with the numerical simulation (a) vs. (c) and (b) vs. (d). The effective Rabi frequency of Floquet Raman transition is estimated to be 0.377 MHz (a) vs. 0.386 MHz (c) and 0.231 MHz (b) vs. 0.240 MHz (d). The frequency of the driving microwave field is $\omega = (2\pi)7.09$ MHz, the other parameters are $\Delta_z = (2\pi)9.92$ MHz, and $\Delta_x = (2\pi)10.12$ MHz.

Analog photon-assisted Raman transition by frequency-modulated driving

Periodic modulation of the trapping potential can lead to an analog of photon-assisted tunneling [3, 4], which e.g. can be implemented in sinusoidally shaken optical lattice or by applying AC electric field in solid-state systems. Here, we analyse the similar analog of photon-assisted phenomena in far-detuned Raman transition. We consider a simple Λ system with the following Hamiltonian

$$H = \omega |e\rangle \langle e| + \mu (|e\rangle \langle g_1| + |e\rangle \langle g_2| + h.c.). \quad (\text{S.26})$$

The transition from the state $|g_1\rangle$ to $|g_2\rangle$ represents a far-detuned Raman transition with an effective transition rate $\Omega_e = \mu^2/2\omega$. The periodic modulation of the energy levels as follows

$$\mathcal{V}(t) = a \cos(\nu t) (|g_1\rangle \langle g_1| - |g_2\rangle \langle g_2|), \quad (\text{S.27})$$

where a and ν represents the amplitude and frequency of the modulation. Define the time-dependent operator

$$\mathcal{K}(t) = \omega t |e\rangle \langle e| + \left(\frac{a}{\nu}\right) \sin(\nu t) (|g_1\rangle \langle g_1| - |g_2\rangle \langle g_2|). \quad (\text{S.28})$$

The effective Hamiltonian can be written as

$$\begin{aligned} \mathcal{H}_{\text{rot}}(t) &= e^{i\mathcal{K}(t)} \mathcal{H}(t) e^{-i\mathcal{K}(t)} + i \frac{\partial e^{i\mathcal{K}(t)}}{\partial t} e^{-i\mathcal{K}(t)} \\ &= g \exp \left\{ i\omega t + i \left(\frac{a}{\nu}\right) \sin(\nu t) \right\} |g_1\rangle \langle e| + g \exp \left\{ i\omega t - i \left(\frac{a}{\nu}\right) \sin(\nu t) \right\} |g_2\rangle \langle e| + h.c. \\ &= g \sum_n \mathcal{J}_n \left(\frac{a}{\nu}\right) e^{i(\omega+n\nu)t} |g_1\rangle \langle e| + g \sum_n \mathcal{J}_n \left(\frac{a}{\nu}\right) e^{i(\omega-n\nu)t} |g_1\rangle \langle e| + h.c. \end{aligned} \quad (\text{S.29})$$

where $\mathcal{J}_n(x)$ is the n -th order Bessel function. When the resonance condition $k\nu = \omega$ is satisfied, with the rotating wave approximation, we only consider the time-independent terms in this Hamiltonian as

$$\mathcal{H}_{\text{eff}} = (-1)^k g' |g_1\rangle \langle e| + g' |g_2\rangle \langle e| + h.c. \quad (\text{S.30})$$

where $g' = g\mathcal{J}_k(\frac{a}{\nu})$. We remark that depending on the value $\frac{a}{\nu}$ one obtains a strong transport or when $\mathcal{J}_k(\frac{a}{\nu}) = 0$ one finds suppressed transport, i.e. dynamical localisation [5, 6]. If k is even (odd), the amplitude of two tunneling term have the same (opposite) value. Assume the initial state is $|g_1\rangle$, the final state at time t can be easily calculated as

$$|\psi_f(t)\rangle = \frac{1 + \cos(\sqrt{2}g't)}{2} |g_1\rangle \mp \frac{1 - \cos(\sqrt{2}g't)}{2} |g_2\rangle - i \frac{\sin(\sqrt{2}g't)}{\sqrt{2}} |e\rangle. \quad (\text{S.31})$$

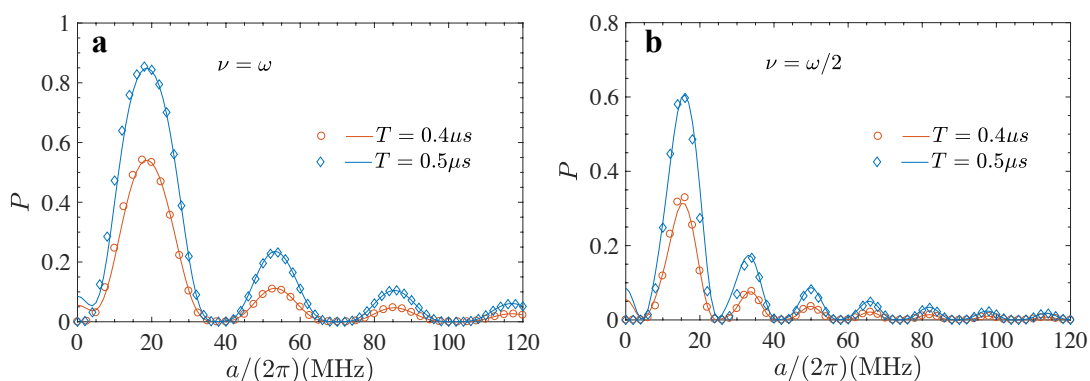


Figure S3: (Color online) The transition probability from the state $|g_1\rangle$ to $|g_2\rangle$ as a function of the amplitude of frequency modulation in a single- (a) and two- photon (b) assisted Raman processes after an evolution time of T . The analytical prediction (\circ and \diamond) in Eq. (S.32) shows good agreement with the numeric simulation. The zeros of the transition probability in both plots correspond to dynamical localisation. The parameters are $\omega = (2\pi)10\text{MHz}$, $\mu = (2\pi)1\text{MHz}$.

The transition probability from the state $|g_1\rangle$ to $|g_2\rangle$ is given by

$$P(t) = \cos^4 \left[\frac{1}{\sqrt{2}} g \mathcal{J}_k \left(\frac{a}{\nu} t \right) \right]. \quad (\text{S.32})$$

At time $t = (\pi/g')$, one can a complete state transfer from $|g_1\rangle$ to $|g_2\rangle$. The value of k is even or odd does not influence the result. The above analytical results agree well with the exact numeric simulation, as shown in Fig.S3, which clearly demonstrate that the photon-assisted Raman transition exhibits significantly enhanced state transfer efficiency.

The analog photon-assisted Raman transition can also appear in Floquet synthetic dimensions. To demonstrate this phenomena, we introduce the following driving field with frequency modulation as

$$V_d(t) = A \sin [\omega t + a \sin(\nu t)]. \quad (\text{S.33})$$

This would lead to the following Floquet Hamiltonian as

$$\begin{aligned} \mathcal{H} = & \sum_{n,\sigma} \left[n(\omega + a \sin(\nu t)) + \frac{\omega_0}{2} \sigma_z \right] |n, \sigma\rangle \langle \sigma, n| + \frac{A\Delta_x}{2\omega_0} \sum_n (|n, +\rangle \langle n+1, +| - |n, -\rangle \langle n+1, -| + h.c.) \\ & + \frac{A\Delta_z}{2\omega_0} \sum_n (|n, +\rangle \langle n+1, -| + |n, -\rangle \langle n+1, +| + h.c.). \end{aligned} \quad (\text{S.34})$$

The above Hamiltonian represents a two-band Wannier-Stark ladder with periodic modulation of lattice potential. Our analysis shows that it is feasible to observe analog photon-assisted Floquet Raman transition in such a driven two-level system, as shown in Fig.4 of main text.

Violation of the traditional adiabatic condition

The adiabatic theorem states that if the Hamiltonian of a system changes slow enough, it will remain in its instantaneous eigenstate [7]. The traditional adiabatic condition is given by [8]

$$\forall m \neq n \quad \left| \frac{\langle m(t) | \dot{n}(t) \rangle}{E_m(t) - E_n(t)} \right| = \left| \frac{\langle m(t) | \dot{H}(t) | n(t) \rangle}{(E_m(t) - E_n(t))^2} \right| \ll 1, \quad (\text{S.35})$$

with $|m(t)\rangle$ and $|n(t)\rangle$ are the instantaneous eigenstates of the time-dependent Hamiltonian $H(t)$, $E_m(t)$ and $E_n(t)$ are the corresponding eigenenergies. For the present Hamiltonian as in Eq.(S.4), the instantaneous eigenstates are $|e(t)\rangle = \cos(\varphi/2) |0\rangle + \sin(\varphi/2) |1\rangle$, and $|g(t)\rangle = -\sin(\varphi/2) |0\rangle + \cos(\varphi/2) |1\rangle$, where $\varphi = \tan^{-1} [(\Delta_x + 2A \sin(\omega t))/\Delta_z]$. The corresponding eigenenergies are $\pm\Omega_0$ with $\Omega_0 = (1/2) [\Delta_z^2 + (\Delta_x + 2A \sin(\omega t))^2]^{1/2}$. The traditional adiabatic condition Eq.(S.35) can be written as

$$\text{QAC}_1 : C_1 = \left| \frac{\langle e(t) | \dot{H}(t) | g(t) \rangle}{(E_e(t) - E_g(t))^2} \right| = \left(\frac{\omega A \Delta_z}{8\Omega_0^3} \right) |\cos(\omega t)| \ll 1, \quad (\text{S.36})$$

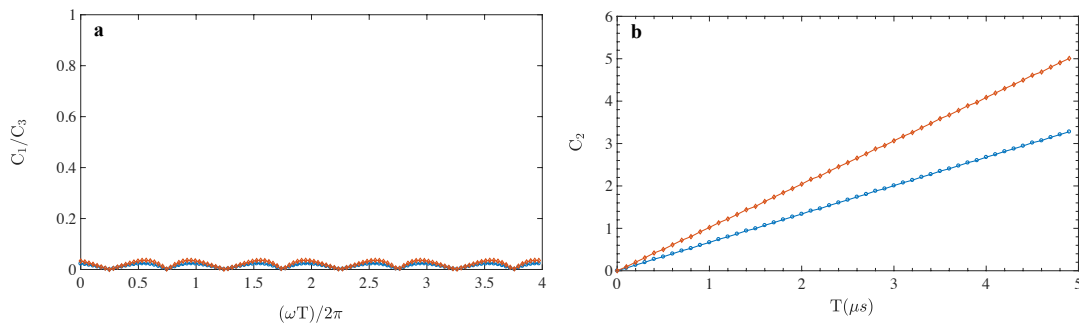


Figure S4: (Color online) C_1/C_3 (a) and C_2 (b) as a function of the evolution time in Floquet Raman transition. The amplitude of the microwave driving field is $A = (2\pi)0.92$ MHz (blue, \circ), $(2\pi)1.35$ MHz (brown, \diamond), and the frequency of the driving microwave field is $\omega = (2\pi)7.09$ MHz, the other parameters are $\Delta_z = (2\pi)9.92$ MHz, and $\Delta_x = (2\pi)10.12$ MHz.

which is neither sufficient nor necessary [9]. Ref. [10, 11] proposed a strong sufficient (but not necessary) condition to guarantee the reliability of adiabatic theorem as follows

$$\text{QAC}_2 : C_2 = \int_0^T \left| \left(\frac{\langle m(t) | \dot{n}(t) \rangle}{E_m(t) - E_n(t)} \right)' \right| dt \ll 1, \quad (\text{S.37})$$

where T is the total evolution time. Another modification of the traditional adiabatic condition is given as follows[13]

$$\text{QAC}_3 : C_3 = \left| \frac{\langle m(t) | \dot{n}(t) \rangle}{E_m(t) - E_n(t) + \Delta_{nm}(t)} \right| \ll 1, \quad (\text{S.38})$$

and Δ_{nm} is defined as

$$\Delta_{nm}(t) = i\langle n(t) | \dot{n}(t) \rangle - i\langle m(t) | \dot{m}(t) \rangle + i \frac{d}{dt} \arg \langle m(t) | \dot{n}(t) \rangle. \quad (\text{S.39})$$

For the present Hamiltonian Eq.(S.4) in our experiment, $\langle g(t) | \dot{g}(t) \rangle = \langle e(t) | \dot{e}(t) \rangle = 0$ and

$$\langle e(t) | \dot{g}(t) \rangle = -\frac{\dot{\varphi}}{2} = -\frac{A\Delta_z\omega \cos(\omega t)}{4\Omega_0^2} \quad (\text{S.40})$$

is always a real number, thus $\Delta_{nm} = 0$, and the condition is equivalent to the traditional adiabatic condition, namely $C_1 = C_3$. It has been experimentally verified in [12] that QAC_1 is neither sufficient nor necessary, and QAC_2 is a strong sufficient condition, while QAC_2 is applicable to the system therein. We plot C_1/C_3 and C_2 in Fig.S4 for the observed Floquet Raman transition processes. It can be seen that our experiment also demonstrates that QAC_1 is not sufficient, while QAC_2 is a strong sufficient condition, which agree with the observation in [12]. Moreover, the result instead shows that QAC_3 is not sufficient, see Fig.S4(a). The present experiment of Floquet Raman transition thus offers a new and more general scenario to gain insights into different formalisms of adiabatic condition [9–11, 13–15].

* These authors contributed equally to this work.

† Electronic address: shaoliang@hust.edu.cn

‡ Electronic address: jianmingcai@hust.edu.cn

- [1] A. Russomanno, G. E. Santoro, *J. Stat. Mech.* **2017**, 103104 (2017).
- [2] E. E. Mendez and G. Bastard, *Physics Today* **46**, 6, 34 (1981).
- [3] A. Eckardt, T. Jinasundera, C. Weiss, and M. Holthaus, *Phys. Rev. Lett.* **95**, 200401 (2005).
- [4] C. Sias, H. Lignier, Y. P. Singh, A. Zenesini, D. Ciampini, O. Morsch, and E. Arimondo, *Phys. Rev. Lett.* **100**, 040404 (2008).
- [5] A. Vaziri and M. B Plenio, *New J. Phys.* **12**, 085001 (2010).
- [6] D. H. Dunlap and V. M. Krenke, *Phys. Rev. B* **34**, 3625 (1986).
- [7] M. Born and V. Fock, *Z. Phys.* **51**, 165 (1928).
- [8] J. J. Sakurai, Jim J. Napolitano, *Modern Quantum Mechanics (2nd Edition)*, World Book Press (2011).
- [9] K.-P. Marzlin and B. C. Sanders, *Phys. Rev. Lett.* **93**, 160408 (2004).
- [10] D. M. Tong, K. Singh, L. C. Kwek, and C. H. Oh, *Phys. Rev. Lett.* **95**, 110407 (2005).
- [11] D. M. Tong, K. Singh, L. C. Kwek, and C. H. Oh, *Phys. Rev. Lett.* **98**, 150402 (2007).
- [12] J.-F. Du, L.-Z. Hu, Y. Wang, J.-D. Wu, M.-S. Zhao, and D. Suter, *Phys. Rev. Lett.* **101**, 060403 (2008).
- [13] J. D. Wu, M. S. Zhao, J. L. Chen, Y. D. Zhang, [arXiv: 0706.0264](https://arxiv.org/abs/0706.0264) (2007).
- [14] A. Ambainis, O. Regev, [arXiv: quant-ph/0411152](https://arxiv.org/abs/quant-ph/0411152) (2004).
- [15] Dafa Li and Man-Hong Yung, *New J. Phys.* **16** 053023 (2014).